Effect of Overlapping Eco-Friendly Cellulose Nanofibrils and Nanoclay Layers on Mechanical and Barrier Properties of Spray-Coated Papers

Maria Luiza Cafalchio de Oliveira
Universidade Federal de Lavras
Seyedmohammad Mirmehdi
Universidade Federal de Lavras
Mário Vanoli Scatolino (mario_paraiso@hotmail.com)
Universidade Federal de Lavras Departamento de Ciencias Florestais https://orcid.org/0000-0002-0412-994X
Mario Guimarães Júnior
Centro Federal de Educação Tecnólogica de Minas Gerais: Centro Federal de Educacao Tecnologica de Minas Gerais
Anand Ramesh Sanadi
University of copenhagen
Renato Augusto Pereira Damasio
Klabin
Gustavo Henrique Denzin Tonoli
Universidade Federal de Lavras

Research Article

Keywords: cellulose nanofibrils, montmorillonite, spray coating, barrier properties, papers.

Posted Date: September 21st, 2021

DOI: https://doi.org/10.21203/rs.3.rs-897414/v1

Abstract

This work proposes to evaluate the effect of spray-coating in papers using eco-friendly cellulose nanofibrils (CNFs) and nanoclay (NC) on mechanical and barrier properties for application as reinforced bags. Sack kraft papers of 60 g m^{-2} (C60) were coated with CNFs + CNFs/NC in 4 layers (L5), 40 g m^{-2} of CNFs + CNFs/NC in 3 layers (L4), 30 g m^{-2} with CNFs/NC in 2 layers (L3) and 10 g m^{-2} of CNFs in 1 layer (L2), and compared to uncoated sack kraft papers with basis weight of 60 g m^{-2} (C60), 80 g m^{-2} (C80) and 120 g m^{-2} (C120). The coated papers L2; L3; L4 and L5 obtained a decrease in water vapor transmission rate (WVTR) of 3.5%; 17%; 14% and 14%, respectively, when compared to C60. Comparing L2 and L3, CNF layer induced lower contact angles on the coated paper than CNF/NC layer. When compared coated papers with C120, it was observed an increase of around 66% in tensile strength for L2, around 44% for L3, and decrease of ~ 18% for L5 coated papers. L4 achieved the same tensile strength (when divided by basis weight) than C120. L2 and L3 coated papers led to the highest values of Young's modulus, with increase of 56% and 38%, respectively, when compared to C60. Spray-coating in the present conditions improved the mechanical and barrier properties of the coated papers, being a possible alternative to produce papers with lower basis weight and using renewable raw materials.

1. Introduction

Paper is one of most widely used materials and has a variety of uses. Kraft paper is produced from wood chips, which are themselves composites, and are due to their high strength, used in packaging applications. Traditionally, the function of packaging is to protect products during transport, storage and commercialization, besides providing information to the consumer about the packed product. Currently, paper is the most important material for packaging industry due to its low price, renewability, recyclability, abundance (Lavoine et al. 2014) and mechanical characteristics such as high strength and flexibility (Afra et al. 2016). However, the use of standard paper in packages is limited to products that do not require some impermeability characteristics. Efforts are ongoing to reduce their water vapor permeability, and several coating techniques have been proposed in literature to modify the paper surface. Among them, the use of different materials, such as fossil source polymers (Reis and Noleto 2015), waxes (Zhang et al. 2014), clays (Mirmehdi et al. 2017), silica nanoparticles (Ogihara et al. 2014), and cellulose nanofibrils (CNF) (Mirmehdi et al. 2018), has been widely reported. Other materials such as biopolymers with antimicrobial additives (Vartiainem et al. 2010), starch to improve optical and mechanical properties (Li et al. 2016), cellulose nanofibrils (CNFs) to improve mechanical strength and barrier properties (Beneventi et al. 2015; Kumar et al. 2016; Afra et al. 2016) and nanoclays (NC) with the purpose of reducing air and water permeability (Mirmehdi et al. 2018; Gaikwad and Seonghyuk 2015; do Lago et al. 2020). These studies show the possibilities to improve different properties of sack paper with the addition of coating layers on the paper surface, creating a multilayer paper with superior properties.

NC is an originally powdered and layered structured material that may improve the barrier properties of polymeric films when properly exfoliated and incorporated. Their interlayer distance are in less than 100

nm when exfoliated. CNFs may form a large network structure of hydrogen bonds due their high aspect ratio and high surface area, and consequently, may increase mechanical strength and decrease water vapor and gas permeability of the paper samples. Notably, NC and CNFs have great potential to be applied in multilayered paper-based packages. Barrier properties of nanoclays and mechanical and barrier properties of CNFs may overcome some challenges of the paper-based packages.

The NC from montmorillonite family is a hydrophilic clay formed by layers of silica tetrahedral and alumina octahedral sheets in a 2:1 ratio (Floody et al. 2009). Due to their low cost and abundance, they have been widely studied for several applications such as a drug-delivery carrier (Jayrajsinh et al. 2017), water treatment (Heidari et al. 2021), composites reinforcement (Moghri et al. 2018), and as coating layers for papers (Majeed et al. 2013). Cellulose fibers can be processed to obtain nanostructures with different properties depending on extraction method and fibers source. There are different kind of cellulose nanostructures obtained from vegetal sources: the fibrillation of cellulose cell walls by mechanical shear forces (wood or non-wood fibers), and/or after chemical or enzymatic treatment. The CNF is composed of amorphous and crystalline regions with an average diameter less than 100 nm and several micrometers in length (Dufresne 2013; Moon et al. 2011; García et al. 2016).

Recent studies reported the production of CNFs from wood (Tonoli et al. 2012; Scatolino et al. 2018; Silva et al. 2021) and some non-wood resources such as agricultural wastes (Petroudy 2017), hemp (Pacaphol and Aht-Ong 2017; Pulikkalparambil et al. 2017), jute (Fonseca et al. 2019; Fonseca et al. 2021), bamboo (Guimarães Jr. et al. 2018), sisal (Krishnan et al. 2015), algae (Chen et al. 2016), cocoa shell (Souza et al. 2018) and bacterial (Corral et al. 2017). Several studies on CNFs have been reported in literature, such as improvement of paper properties (Afra et al. 2016; Herrera et al. 2015; Lavoine et al. 2016), in medical applications (Sundberg et al. 2013), nanoparticle carriers (Scatolino et al. 2019), electronic devices (Jung et al. 2015), reinforcement in polymeric matrices (Volk et al. 2015; Chinnama et al. 2016), fiber-cement composites (Fonseca et al. 2021) and packaging materials (Missoum et al. 2013; Scatolino et al. 2017). The aim of this paper was to evaluate the effect of spray coating for producing different layers composed of CNFs and NC, varying their order and mixture composition of CNFs + NC, on tensile and barrier properties of the coated sack papers.

2. Materials And Methods

2.1 Material obtainment

The paper used as the substrate for coating was the commercial sack kraft paper (extensible) with nominal weight basis of 60 g m^{-2} (C60), 80 g m^{-2} (C80) and 120 g m^{-2} (C120). Sheets of commercial eucalyptus bleached kraft pulp (Klabin S/A, SP-Brazil), was the source to produce the CNFs. The nanoclay (NC) used in the coatings (mixed to CNFs) were obtained from Sigma-Aldrich Inc. NC is considered as a hydrophilic material from bentonites family ($H_2Al_2O_6Si$) (Sigma-Aldrich Inc.) and was used along with CNF suspension.

2.2. Production of the CNFs

Eucalyptus bleached kraft pulp was hydrated and dispersed for 24 h in deionized water in 2% wt concentration and dispersed under mechanical stirring at 1000 rpm for 3 h. The suspension was submitted to 30 passages through the fibrillator SuperMasscolloider (Masuko Sangyo MKCA6-3, Japan), which has a fixed and a rotating disc (1500 rpm) that promote the cellulose fibrillation by shear forces, resulting on a gelatinous aspect. The fibrillation process followed the guidelines suggested in previous works (Tonoli et al. 2016; Guimarães Jr et al. 2015; Bufalino et al. 2015; Dias et al. 2019; Durães et al. 2020). The fibrillation breaks the bonds between elementary fibers and fibers bundles by shear forces, resulting on CNF dispersion. The representative scheme of fibrillation process can be observed in Figure 1.

2.3. Preparation of the NC

A small fraction of 3% wt of hydrophilic NC from bentonites family was dispersed in deionized water (w/w) and magnetically stirred for 24 h. The mixture was sonified for 10 min following the methodology described in Bardet et al. (2015). This step was important in exfoliating the NC plates and facilitate its incorporation in the coating mixture (Figure 2) besides to promote better adhesion to the paper used as substrate.

2.4. CNF and CNF/NC solutions

The CNFs and CNF/NC solutions were prepared in order to spray it on the paper surface. For CNF solution, 1.4% wt CNF was added to deionized water, and then stirred at 900 rpm for 30 min. CNF/NC solution was prepared adding 1.0% of exfoliated NC and 1.4% of CNFs in deionized water, and stirred at 900 rpm for 30 min in order to intercalate the nanoclay plates in the cellulosic matrix. Some studies have shown the suitable interaction of polymers and inorganic clays (Gabr et al. 2013). A good exfoliated nanoclay can be intercalated in nanocellulosic matrix, allowing a close interaction with the nanocellulose net (Gaikwad and Seonghyuk 2015).

2.5. Experimental setup for the spray coating

CNFs and CNF/NC suspensions were sprayed onto paper, with basis weight 60 g m^{-2}, using a laboratory assembled spray coater (Figure 3A) in multiple layers. Variables and parameters used in this process were pressure of 0.4 MPa, for 30 s of spraying time and 30 cm of distance between spray nozzle and substrate. According to Shanmugam et al. (2017), the operational range of CNF suspension concentration for spraying coating is between 1% and 2%. Below 1% wt, the suspensions are too dilute and does not form a continuous and homogenous layer over the substrate, and high concentrations of CNF suspension (above 2.0% wt) are too viscous to be applied by the spray technique. Based on that, suspensions with 1.4% wt of CNFs and 1.0% of nanoclay were prepared along with suspensions of only 1.4% of CNFs.

The paper sheets were coated over a vacuum dewatering setup to obtain a consistent removal of the water from the coated papers before oven drying. After each coating step, papers were oven-dried at 100±5 °C for 3 h. The different paper treatments are depicted in Figure 3B. The samples were conditioned at 20 °C and 50% of relative humidity (RH) prior to characterizations.

2.6 Production of CNFs and CNF/NC films

Films were produced from the CNFs and CNFs/NC by casting method. An aliquot of 40 ml of CNF suspensions (1.4% wt) and CNFs/NC (1.4% of CNFs and 1.0% of NC, both wt) was deposited on petri dishes and oven dried at 60 °C for 48 h. These concentrations of suspensions were calculated aimed to produce films with basis weight similar to that applied as layer on the papers which were around 20 g m^{-2} for CNF/NC films and 10 g m^{-2} for CNF films.

2.7.Thickness and basis weight of the papers and films

The thickness of the papers was measured before and after the coating process using a digital micrometer, according to the ASTM D645-97 (2007) standard. Basis weight was determined using samples with diameter of 16 mm, previously oven dried at 100 ± 3 °C and weighed according to the ASTM D 646-96 (1996) standard. Thickness and basis weight of the films were also calculated. The basis weight was measured before and after the spray coating process according to Eq. 1.

$$Bw = M / A \quad (1)$$

Where: Bw is the basis weight (g m^{-2}); M is the mass of the sample (g); A is the area of the sample (m^2).

2.8 Tensile properties of the papers and films

Tensile properties were determined using a universal testing machine MTS Landmark servo hydraulic test system, according to ASTM D 828-97 (2002) standard. The specimens were cut parallel to the fiber's direction of the paper. Data were acquired using the Station Manager software. The dimension required for the specimens was 20 mm in width and around 100 mm in length. The distance between the grip clamping zones was 50 mm and the dislocation rate was 14.1 mm/min. Tensile strength, Young's modulus and elongation at break of the films and papers were divided by the basis weight in order to normalize the results. The average value for each property was obtained by the average of five samples.

2.9. Water vapor transmission rate of the papers

The water vapor transmission rate (WVTR) measurements were performed according to the method described in ASTM E96 / E96M-16 (2016) standard, followed by Guimarães Jr et al. (2015). The test was conducted in a laboratorial apparatus (Figure 4) composed of permeability cells with relative humidity of 0% placed inside a desiccator with of relative humidity of 75%. A saline NaCℓ solution was used to keep the relative humidity at 75% into the desiccator. The permeability cells were filled with silica in order to keep the initial humidity at 0%. The samples of films and papers were placed in the cap of the cells. In

addition, reference cells were allocated into the apparatus to reduce the experimental error; reference 1 - cell with aluminum sheet instead of the paper sample and reference 2 - cell without silica. The mass was daily monitored for eight days. The results of WVTR were obtained by the average of five samples per treatment.

2.10. Scanning electron microscopy of the papers

Surface and cross section of the papers were assessed by scanning electron microscopy (SEM) in order to evaluate the structure of the layers deposed on the paper surface. A Zeiss LEO EVO 40 XVP microscope with secondary electron detector and accelerating voltage of 20 kV was used and the samples were coated with gold before the analysis by sputter coating technique.

2.11 Contact angle of the papers and films

The contact angle of the papers and films substrates was carried out by depositing drops of water on the samples surface. A Kruss Advance equipment, equipped with a CCD camera working at up to 200 images per second was used for the measurements. Results were obtained by an average of six experimental contact angles, detected in the first microseconds where the drops become stable on the sample surface.

3. Results And Discussion

3.1. Morphological characterization of the coated papers

SEM surface micrographs show presence of pores in the surface of uncoated paper C60 (Figure 5a and b). Surfaces of uncoated C80 and C120 sack kraft paper showed the similar attributes as C60, nevertheless, the pictures are not presented here. A reduction of pores was observed with the deposition of the coating layers (Figures 5c to h), especially in L2 and L3, in which the coatings led to a smooth and uniform layer over the paper substrate. On the other hand, SEM surface images of L5 (Figures 5g and h) showed a heterogeneous coating, with a porous and rough surface due to the large amount of coating material on the paper surface. Samples of the coated paper L4 are not shown here as the external surfaces are the same shown for L2 (Figures 5c and d).

SEM images of the papers cross section showed that spraying layers of CNFs and CNFs/NC on the paper surfaces increased the thickness and also creating a tortuous pathway for any substance to cross the paper. The uncoated paper C60 showed many micropores throughout the cross section, which was extended to all coated papers (Figure 6). The coated papers designated as L2, L3, L4 and L5 had more compact layers (external or internal) due to the coatings composed by CNFs or CNFs/NC.

3.2 Thickness and basis weight of the papers and films

Thin CNF layers are sufficient to change the surface properties of the coated sack kraft paper, while thicker and uniform layers are required to change barrier properties (Brodin et al. 2014). The CNF and CNF/NC layers were deposited on the sack kraft papers by the spraying method, and the increase of

thickness and basis weight were proportional to the number of layers deposited. Each layer of CNFs or CNFs/NC increased the basis weight of the paper by about 10 g m^{-2} - 20 g m^{-2} (Table 1).

The films produced from pure CNFs and CNFs/NC presented similar basis weight than each coating layer deposited on the coated papers (L2, L3, L4, and L5 treatments).

3.3 Tensile strength of the multilayered papers

The coated papers had different values of basis weight, therefore the mechanical results were also divided by the basis weight value of the correspondent treatment (Table 2), in order to normalize the comparison among the properties of the papers. Table 3 presents the mechanical properties of the films produced with CNFs and CNFs/NC.

CNFs usually form a network in nanoscale and have more fibrils per gram of material when compared to fibers in microscale, and consequently can form more inter-fibril bonds (Brodin et al. 2014). All the papers decreased in tensile strength values as compared to C60 (uncoated), when analyzing the normalized values (divided by basis weight). Lavoine et al. (2014) studied the mechanical properties of CNF coated papers by two methods of coating, bar coating and size press. The two methods studied revealed higher tensile strength for uncoated paper than CNF coated papers. The authors associated this behavior to four factors: (1) non-uniformity of coating layers; (2) insufficient coat weight of CNFs to promote improvements on mechanical properties; (3) CNFs did not penetrate into paper structure; and (4) greater amount of water penetrated in the paper structure instead CNFs.

Sack kraft paper (C120 = 120 g m^{-2}) is usually used for production of packages for grains and seeds weighing up to about 60 kg. Then, the present results observed for coated papers were comparable to C120 uncoated paper. There was an increase of around 66% in tensile strength for L2 and around 44% for L3, when compared to C120. The L4 coated paper showed the same average value of tensile strength presented by C120. On the other hand, normalized tensile strength of L5 was around 19% lower than C120. The coating process performed for preparation of L5 treatment subjected the substrate to the highest number of wetting/drying cycles during the coating application. Successive wetting/drying cycles may induce some hornification process to the paper fibers. Swelling occurs in the cell volume when cellulose fiber is placed in suspension with water, and when they are dried, their volume shrinks. However, when these fibers were re-suspended in water, the original volume is not recovered, decreasing the fibers capacity of water retention. Moreover, when water is removed from the fibers, part of cell wall collapse, increasing inter-fibrillar bonding, forming irreversible and partially reversible hydrogen bonds (Ferreira et al. 2017). Besides, the pore volume is reduced modifying the pore size distribution of the paper (Hubbe et al. 2007), which leads to the increase of stiffness of the paper fibers. Cao et al. (1999) compared papers produced from once dried fibers and never dried fibers, concluding that the once dried fibers was less conformable and, consequently the paper made from them resulted in lower strength. The same behavior was observed for the L5 coated paper of the present work.

Furthermore, the high standard deviation obtained for basis weight of the L5 paper suggests a heterogeneous coating that did not increase the tensile strength of the paper. Afra et al. (2016) reported an increase in tensile index for CNF coated papers proportional to the added CNF basis weight. Syverud and Stenius (2009) studied mechanical properties of CNF coated paper and reported 6% of decrease on tensile index with 2 g m^{-2} of CNF addition compared to uncoated paper. However, the authors reported that application of thicker layers (4 and 8 g m^{-2}) promoted 6% and 14% of tensile index increase, respectively. All coated papers showed an increase of Young's modulus in relation to the uncoated papers. Similar result was reported in Afra et al. (2016), with CNF coating layers on paper sheets, relating that stiffness is proportional to the applied CNF basis weight. On the other hand, Lavoine et al. (2014) observed a decrease in Young's modulus after CNF application on the paper. The authors observed a decrease of around 20 - 45% in Young's modulus with the coating composed of 3 - 14 g m^{-2} of CNFs. The values of Young's modulus were divided by the basis weight to normalize the comparison among treatments. In this work, spraying a layer of 10 g m^{-2} of CNFs (L2) and around 20 g m^{-2} of CNFs/NC (L3) resulted in a great increase in Young's modulus (56% for L2 and 28% for L3). In other cases, the application of greater basis weight of CNFs/NC (57 g m^{-2} for L5 and 42 g m^{-2} for L4), a considerable decrease in Young's modulus (30% and 7% for L5 and L4, respectively) was observed, in comparison to C60. The elongation at break for the coated papers reduced after the coatings of around 60%, 50%, 50%, and 40% for L2, L3, L4 and L5, respectively, in relation to uncoated papers. Sack kraft paper is constituted by many micro wrinkles that confers extensibility properties to the paper. In contrast, CNFs and CNFs/NC form a layer that restrict the extensibility and decrease elongation of the paper. Agglomerated NC layers are responsible for stress concentrations in the paper and decreases the elongation at break (Gabr et al. 2013). Figures 7 and 8 show the evolution of stress-elongation of the samples during the tensile test. Stress x specific elongation (mm/mm) of uncoated papers C60, C80 and C120 showed maximum stress of around 35 MPa.

L4 and L5 coated papers presented curves with a second mechanical performance due to the presence of the deposited layers. During the tensile loading, the break of different layers do not occur at the same time. The layers composed by CNFs and CNFs/NC, which are stiffer, are responsible for the initial mechanical performance (first rupture), and then the paper substrate is finally mechanically broken (Figure 9).

3.3 Contact angle of the papers and films

Measuring the contact angle of a water drop on the paper substrate surface gives an insight into the hydrophobicity of the surface, which can be defined as the tendency of a water drop not to spread on the substrate. CNF coating layers induced the decrease of the contact angle (87°) for L2 coated papers, in comparison to uncoated paper C60 (111°). However, this difference was not observed for the L3 treatment that was coated with CNFs and CNFs/NC (110°) (Figure 10). Greater basis weight did not indicate lower hydrophobicity for the papers C80 and C120.

The film produced from CNFs/NC showed greater contact angle in relation to the CNF film, confirming that CNF/NC coating seems to be more effective for decreasing hydrophobicity. The hydrophilic nature of CNFs, especially after the cell wall fibrillation process is a determining factor in its application as paper coating. NC are formed by layers of tetrahedral silica sheets and alumina octahedral sheets containing Ca^{2+} or Na^{+} that have the capacity to adsorb water (Paiva et al. 2008; Silva and Ferreira, 2008), whereas when adequately dispersed into the polymeric matrices, the nanoclays presents good barrier properties (Gabr et al. 2013; Gaikwad and Seonghyuk 2015). It was observed that the L5 coated paper resulted in different contact angles, when evaluating the internal and external faces of the coated paper, even if the layer composition is the same on both sides. This may have occurred due to some heterogeneity of the layers deposition on the paper surface, with regions with excessive deposition of coating, and others with insufficient coating. The surface roughness of the different deposited layers may also have some influence on the hydrophobicity. Although L3 and L5 have a rougher surface compared to L2, they tended to have greater contact angles and this was probably due to the presence of NC, which sometimes caused agglomerations and surface granularity. Low values of contact angles (<90°) indicate that the material have lower hydrophobicity, while high contact angles (>90^{o}) indicate low hydrophobicity (Yuan and Lee 2013).

3.4 Water vapor transmission rate of the films and papers

Films produced with CNFs/NC showed less vapor transmission compared to films produced with only CNFs (Figure 11). The addition of NC to the composition of the CNF films resulted in reduction of around 11% on the WVTR evaluated in the study. Generally, the incorporation of NC into CNFs is expected to retard the degradation process, due to lower moisture present due to the formation of silicate layers as a protective barrier, and/or via inducing obstacles that could delay the passage of water vapor (Leszczyńska et al. 2007). Literature data shows WVTR values ranging between 234 – 332 g m^{-2} day^{-1} for films produced with CNFs/NC (Rodionova et al. 2011; Lu et al. 2015).

When successfully dispersed in polymeric matrix, NC can hinder the diffusion trough the matrix due the tortoise path created by exfoliated plates that could improve barrier properties (Gaikwad and Seonghyuk 2015). The NC grains adsorb water, which expand and form barrier layers against vapor transmission (Vartiainen et al. 2010). As previously discussed, CNFs are hydrophilic materials with high aspect ratio and strong capacity to form close networks (Dufresne 2013) that may promote the decrease of WVTR. CNF/NC coating layers led to lower WVTR than pure CNF coating layers. SEM micrographs (Figure 5a to h) demonstrated that the CNF and CNF/NC layers reduced the porosity of the paper substrate, contributing to WVTR reduction. Reduction of WVTR was observed for all multilayered papers when compared to uncoated samples (C60, C80 and C120). Analyzing the uncoated papers with different basis weight, it is noted that greater basis weights did not result in lower WVTR, indicating that the real influence on this property is exerted by the composition of the paper/film and coating agent. The coating with 10 g m^{-2} of CNFs on 60 g m^{-2} sack kraft paper (L2 coated paper) promoted a decrease of around 4% in WVTR in relation to C60, leading to a homogeneous less porous surface that may be further coated with other hydrophobic and barrier agents in the future.

L3, L4 and L5 presented lower WVTR compared to L2 and uncoated papers (C60, C80 and C120). In this case, the greater number of layers deposited on the paper surface may have created more obstacles against the vapor passage. Results showed that L3 coated paper led to a reduction of around 17% for WVTR in relation to the 60 g m^{-2} uncoated paper (C60). Additionally, L3 led to the greater contact angle among all the coated papers (see Fig. 15), which means a better combination of layers for this treatment composition, including for mechanical properties. The coated papers L4 and L5 presented a reduction of around 14% for WVTR in comparison to the reference uncoated paper (C60).

4. Conclusion

Commercial sack kraft papers were coated with overlapping layers of CNFs and CNFs/NC and were evaluated through their mechanical and barrier properties. Coated papers (except L2 treatment) which consists of only CNF layers, showed more efficient water vapor barrier when compared to the uncoated samples. SEM surface images of surface and cross-sections showed that the addition of CNFs and CNFs/NC reduced the paper surface porosity. The addition of CNFs and CNFs/NC also increased the hydrophobicity of the surface of coated papers when compared to control uncoated papers (C60, C80 and C120). The highest values of tensile strength and Young's modulus were observed for coatings with 10 g m^{-2} of CNFs (L2) and 30 g m^{-2} of CNFs and CNFs/NC (L3). Higher number of layers (4 to 5 layers) applied by spraying in the present conditions seems to be detrimental to mechanical strength and surface properties, and incremental to barrier properties. This is probably due to the challenges of the spray coating technology with just CNF and NC suspensions. The challenges are related to the hornification effect of the fibers in the coated samples when subjected to high number of wetting-drying cycles during the CNF/NC application, for the drying processing of the coated and multilayered papers. This work shows the high potential of CNFs and NC as coatings in packaging paper and the key is to obtain sufficient exfoliation of NC, following by good dispersion of of CNFs and CNFs/CN. Further developments and optimizations on spray coating techniques or other application methods should significantly improve the mechanical and barrier properties of the coated papers for packaging using lower basis weight papers.

Declarations

Conflict of interest statement

The authors confirm that there is no conflict of interest regarding the submission.

References

1. Afra E, Mohammadnejad S, Saraeyan A (2016) Cellulose nanofibils as coating material and its effects on paper properties. Progr Organic Coat 101: 455–460.
2. Andrade R, Skurtys O, Osorio F, Zuluaga R, Gañán P, Castro C (2014) Wettability of gelatin coating formulations containing cellulose nanofibers on banana and eggplant epicarps. LWT- Food Sci

Technol 58: 158–165.

3. American Society for Testing and Materials - ASTM D645M-97 (2007) Standard Test Method for Thickness of Paper and Paperboard (Withdrawn 2010). ASTM International, West Conshohocken, PA, USA.
4. American Society for Testing and Materials - ASTM D646-96 (1996) Standard Test Method for Grammage of Paper and Paperboard (Mass Per Unit Area). ASTM International, West Conshohocken, PA, USA.
5. American Society for Testing and Materials - ASTM D828-97 (2002) Standard Test Method for Tensile Properties of Paper and Paperboard Using Constant-Rate-of-Elongation Apparatus (Withdrawn 2009). ASTM International, West Conshohocken, PA, USA.
6. American Society for Testing and Materials - ASTM E96/E96M-16 (2016) Standard Test Methods for Water Vapor Transmission of Materials. ASTM International, West Conshohocken, PA, USA.
7. Beneventi D, Chaussy D, Curtil D, Zolin L, Gerbaldi C, Penazzi N (2014) Highly porous paper loading with microfibrillated cellulose by spray coating on wet substrates. Ind Eng Chem Res 53: 10982-10989.
8. Brodin FW, Gregersen ØW, Syverud K (2014) Cellulose nanofibrils: Challenges and possibilities as a paper additive or coating material - A review. Nord Pulp Pap Res J 29: 156–166.
9. Bufalino L, de Sena Neto AR, Tonoli GHD, de Souza Fonseca A, Costa TG, Marconcini, JM, Colodette JL, Labory CRG, Mendes LM (2015) How the chemical nature of Brazilian hardwoods affects nanofibrillation of cellulose fibers and film optical quality. Cellulose 22: 3657-3672.
10. Calcagno CIW (2007) Study of the morphology, crystallization behavior and mechanical properties of PET and PP / PET nanocomposites with montmorillonite. Thesis, Federal University of Rio Grande do Sul.
11. Chen YW, Lee HV, Juan JC, Phang Siew-Moi (2016) Production of new cellulose nanomaterial from red algae marine biomass Gelidium elegans. Carbohyd Polym 151: 1210–1219.
12. Chinnama PR, Mantravadia R, Jimeneza JC, Dikinb DA, Wundera SL (2016) Lamellar, micro-phase separated blends of methyl cellulose and dendritic polyethylene glycol. Carbohyd Polym 136: 19-29.
13. Chinga-Carrasco G, Kuznetsova N, Garaeva M, Leirset I, Galiullina G, Kostochko A, Syverud K (2012) Bleached and unbleached MFC nanobarriers: properties and hydrophobisation with hexamethyldisilazane. J Nanopart Res 14: 1-10.
14. Corral ML, Cerrutti P, Vázquez A, Califano A (2017) Bacterial nanocellulose as a potential additive for wheat bread. Food Hydrocol 67: 189-196.
15. Dias MC, Mendonça MC, Damásio RAP, Zidanes UL, Mori FA, Ferreira SR, Tonoli GHD (2019) Influence of hemicellulose content of *Eucalyptus* and *Pinus* fibers on the grinding process for obtaining cellulose micro/nanofibrils. Holzforsch 73: 1035–1046.
16. do Lago RC, de Oliveira ALM, Dias MC, de Carvalho EEN, Tonoli GHD, Vilas Boas EVB (2020) Obtaining cellulosic nanofibrils from oat straw for biocomposite reinforcement: Mechanical and barrier properties. Ind Crop Prod 148: 112264.

17. Dufresne A (2013) Nanocellulose: A new ageless bionanomaterial. Materials Today 16: 220–227.
18. Durães AFS, Moulin JC, Dias MC, Mendonça MC, Damásio RAP, Thygesen LG, Tonoli GHD (2020) Influence of chemical pretreatments on plant fiber cell wall and their implications on the appearance of fiber dislocations. Holzforsch 74:949-955.
19. Eichhorn SJ, Dufresne A, Aranguren M et al (2010) Review: Current international research into cellulose nanofibres and nanocomposites, J Mater Sci 45: 1-33.
20. Ferreira SR, Silva F de A, Lima PRL, Toledo Filho RD (2017) Effect of hornification on the structure, tensile behavior and fiber matrix bond of sisal, jute and curauá fiber cement based composite systems. Const Build Mat 139: 551–561.
21. Floody MC, Theng BKG, Reyes P (2009) Natural nanoclays: applications and future trends - a Chilean perspective. Clay Miner 1: 161– 176.
22. Fonseca AS, Panthapulakkal S, Konar SK, Sain M, Bufalino L, Raabe J, Miranda IPA, Martins MA, Tonoli GHD (2019) Improving cellulose nanofibrillation of non-wood fiber using alkaline and bleaching pre-treatments, Ind Crop Prod 131: 203-212.
23. Fonseca CS, Silva TF, Silva MF, Oliveira IRC, Mendes RF, Hein PRG, Mendes LM, Tonoli GHD (2016) *Eucalyptus* cellulose micro/nanofibrils in extruded fibercement composites. Cerne 22: 59-68.
24. Fonseca CS, Scatolino MV, Silva LE, Martins MA, Guimarães Júnior M, Tonoli GHD (2021) Valorization of Jute Biomass: Performance of Fiber–Cement Composites Extruded with Hybrid Reinforcement (Fibers and Nanofibrils). Waste Biomass Valor. Avaliable at: https://link.springer.com/article/10.1007/s12649-021-01394-1 (Accessed 21 May 2021).
25. Gabr MH, Phong NT, Abdelkareem MA, Okubo K, Uzawa K, Kimpara I, Fujii T (2013) Mechanical, thermal, and moisture absorption properties of nano-clay reinforced nano-cellulose biocomposites. Cellulose 20: 819–826.
26. Gaikwad KK, Seonghyuk KO (2014) Overview on in Polymer-Nano Clay Composite Paper Coating for Packaging Application. J Mater Sci Eng 4: 1–5.
27. García A, Gandini A, Labidi J, Belgacem N, Bras J (2016) Industrial and crop wastes: A new source for nanocellulose biorefinery. Ind Crop Prod 93: 26-38.
28. Guimarães Jr M, Botaro VR, Novack KM, Flauzino Neto WP, Mendes LM, Tonoli GHD (2015) Preparation of cellulose nanofibrils from bamboo pulp by mechanical defibrillation for their applications in biodegradable composites. J Nanosci Nanotechnol 15: 6751-6768.
29. Guimarães Jr M, Teixeira FG, Tonoli GHD (2018) Effect of the nano-fibrillation of bamboo pulp on the thermal, structural, mechanical and physical properties of nanocomposites based on starch/poly(vinyl alcohol) blend. Cellulose 25: 1823–1849.
30. Herrera MA, Sirviö JA, Mathew AP, Oksman K (2016) Environmental friendly and sustainable gas barrier on porous materials: Nanocellulose coatings prepared using spin- and dip-coating. Mater Design 93: 19–25.
31. Iwamoto S, Nakagaito AN, Yano H (2007) Nano-fibrillation of pulp fibers for the processing of transparent nanocomposites. Appl Phys A-Mater 89: 461-466.

32. Jayrajsinh S, Shankar G, Agrawal YK, Bakre L (2017) Montmorillonite nanoclay as a multifaceted drug-delivery carrier: A review. J Drug Deliv Sci Technol 39: 200–209.
33. Jung YH, Chang Tzu-Hsuan, Zhang H, Yao C, Zheng Q, Yang VW, Mi H, Kim M, Cho SJ, Park Dong-Wook (2015) High-performance green flexible electronics based on biodegradable cellulose nanofibril paper. Nat commun 6: 1-11.
34. Heidari A, Sayadi MH, Atigh ZBQ (2021) Comparative study of different materials (drinking water treatment sludge, nanoclay, and modified nanoclay) for simultaneous removal of hexavalent chromium and lead. Int J Environ Sci Technol. Avaliable at https://doi.org/10.1007/s13762-020-03074-4
35. Hubbe MA, Rojas OJ, Lucia LA, Jung TM (2007) Consequences of the nanoporosity of cellulosic fibers on their streaming potential and their interactions with cationic polyelectrolytes. Cellulose 14: 655-671.
36. Krishnan KA, Jose C, Rohith KR, George KE (2015) Sisal nanofibril reinforced polypropylene/polystyrene blends: Morphology, mechanical, dynamic mechanical and water transmission studies. Ind Crop Prod 71: 173–184.
37. Kumar V, Elfving A, Koivula H, Bousfield D, Toivakka M (2016) Roll-to-Roll Processed Cellulose Nanofiber Coatings. Ind Engin Chem Res 55: 3603–3613.
38. Lavoine N, Desloges I, Khelifi B, Bras J (2014) Impact of different coating processes of microfibrillated cellulose on the mechanical and barrier properties of paper. J Mater Sci 49: 2879–2893.
39. Lavoine N, Guillard V, Desloges I, Gontard N, Bras J (2016) Active bio-based food-packaging: Diffusion and release of active substances through and from cellulose nanofiber coating toward food-packaging design. Carbohyd Polym 49: 40–50.
40. Leszczyńska A, Njuguna J, Pielichowski K, Banerjee JR (2007) Polymer/montmorillonite nanocomposites with improved thermal properties: part II. Thermal stability of montmorillonite nanocomposites based on different polymeric matrixes. Thermochim Acta 454: 1–22.
41. Li T, Fan J, Chen W, Shu J, Qian X, Wei H, Wang Q, Shen J (2016) Coaggregation of mineral filler particles and starch granules as a basis for improving filler-fiber interaction in paper production. Carbohyd Polym 149: 20–27.
42. Lin J, Yu L, Tian F, Zhao N, Li X, Bian F, Wang J (2014) Cellulose nanofibrils aerogels generated from jute fibers. Carbohyd Polym 109: 35–43.
43. Lu P, Xiao H, Pan Y (2015) Improving Water Vapor Barrier of Green-Based Nanocellulose Film via Hydrophobic Coating. World scientific 2014 International Conference on Materials Science and Energy Engineering (CMSEE 2014) - Mater Sci Energ Eng (CMSEE 2014) - 148–153.
44. Majeed K, Jawaid M, Hassan A, Abu Bakar A, Abdul Khalil HPS, Salema AA, Inuwa I (2013) Potential materials for food packaging from nanoclay/natural fibres filled hybrid composites. Mater Des 46: 391–410.

45. Mirmehdi S, Hein PRG, Sarantópoulos CIGL, Dias MV, Tonoli GHD (2018) Cellulose nanofibrils/nanoclay hybrid composite as a paper coating: effects of spray time, nanoclay content and corona discharge on barrier and mechanical properties of the coated papers. Food Packaging and Shelf Life. 15:87-94
46. Missoum K, Martoïa F, Belgacem MN, Bras J (2013) Effect of chemically modified nanofibrillated cellulose addition on the properties of fiber-based materials. Ind Crop Prod 48: 98–105.
47. Moghri M, Garmabi H Zanjanijam AR (2018) Prediction of barrier properties of HDPE/PA-6/nanoclay composites by response surface approach: effects of compatibilizer type and the contents of nanoclay, PA-6 and compatibilizer. Polym Bullet 75: 2751–2767.
48. Moon RJ, Martini A, Nairn J, Simonsen J, Youngblood J (2011) Cellulose nanomaterials review: structure, properties and nanocomposites. Chem Soc Rev 7:3369-4260.
49. Pääkkö M, Ankerfors M, Kosonen H, Nykänen A, Ahola S, Österberg M et al. (2007) Enzymatic hydrolysis combined with mechanical shearing and high-pressure homogenization for nanoscale cellulose fibrils and strong gels. Biomacromolecules 8: 1934–1941.
50. Pacaphol K, Aht-Ong D (2017) Preparation of hemp nanofibers from agricultural waste by mechanical defibrillation in water. J Clean Prod 142: 1283–1295.
51. Paiva LB de, Morales AR, Díaz FRV (2008) Organophilic clays: characteristics, preparation methods, intercalation compounds and characterization techniques. Cerâmica 54: 213-226.
52. Petersson L, Oksman K, Mathew AP (2006) Biopolymer based nanocomposites: Comparing layered silicates and microcrystalline cellulose as nanoreinforcement. Compos Sci Technol 66: 2187-2196.
53. Petroudy SRD, Garmaroody ER, Rudi H (2017) Oriented Cellulose Nanopaper (OCNP) based on bagasse cellulose nanofibrils. Carbohyd Polym 157: 1883–1891.
54. Pulikkalparambil H, Parameswaranpillai J, George JJ, Yorseng K, Siengchin S (2017) Physical and thermo-mechanical properties of bionano reinforced poly (butylene adipate-co-terephthalate), hemp/CNF/Ag-NPs composites. AIMS Mater Sci 4: 814–831.
55. Rodionova G, Lenes M, Eriksen O, Gregersen O (2011) Surface chemical modification of microfibrillated cellulose: improvement of barrier properties for packaging applications. Cellulose 18:127–134
56. Scatolino MV, Bufalino L, Mendes LM, Guimarães Júnior M, Tonoli GHD (2017) Impact of nanofibrillation degree of eucalyptus and Amazonian hardwood sawdust on physical properties of cellulose nanofibril films. Wood Sci Technol 51: 1095–1115.
57. Scatolino MV, Dias MC, Silva DW, Bufalino L, Martins MA, Piccoli RH, Tonoli GHD, Londero AA, Neto VO, Mendes LM (2019) Tannin-stabilized silver nanoparticles and citric acid added associated to cellulose nanofibrils: effect on film antimicrobial properties. SN Appl Sci 1: 1243.
58. Scatolino MV, Fonseca CS, da Silva Gomes M, Rompa VD, Martins MA, Tonoli GHD, Mendes LM (2018) How the surface wettability and modulus of elasticity of the Amazonian paricá nanofibrils films are affected by the chemical changes of the natural fibers. Eur J Wood Wood Prod 76: 1581–1594.

59. Shanmugam K, Varanasi S, Garnier G, Batchelor W (2017) Rapid preparation of smooth nanocellulose films using spray coating. Cellulose 24: 2669–2676.
60. Silva ARV, Ferreira HC (2008) Bentonite clays: concepts, structures, properties, industrial uses, reserves, production and nationals and internationals producers/suppliers. Revista Eletrônica de Materiais e Processos 3: 26–35.
61. Silva LE, dos Santos AA, Torres L, McCaffrey Z, Klamczynski A, Greggory G, Sena Neto AR, Wood D, Williams T, Orts W, Damásio RAP, Tonoli GHD (2021) Redispersion and structural change evaluation of dried microfibrillated cellulose. Carbohyd Polyme 1: 117165.
62. Siró I, Plackett, D (2010) Microfibrillated cellulose and new nanocomposite materials: A review. Cellulose 17: 459–494.
63. Syverud K, Stenius P (2009) Strength and barrier properties of MFC films. Cellulose 16: 75–85.
64. Tonoli GHD, Teixeira EM, Corrêa AC, Marconcini JM, Caixeta LA, Pereira-da-Silva MA, Mattoso LHC (2012) Cellulose micro/nanofibres from *Eucalyptus* kraft pulp: Preparation and properties. Carbohyd polym 89: 80-88.
65. Tonoli GHD, Holtman KM, Glenn G et al. (2016) Properties of cellulose micro/nanofibers obtained from eucalyptus pulp fiber treated with anaerobic digestate and high shear mixing. Cellulose 23: 1239–1256.
66. Vartiainen J, Tammelin T, Pere J, Tapper U, Harlin A (2010) Biohybrid barrier films from fluidized pectin and nanoclay. Carbohyd Polym 82: 989-996.
67. Volk N, He R, Magniez K (2015) Enhanced homogeneity and interfacial compatibility in melt-extruded cellulose nano-fibers reinforced polyethylene via surface adsorption of poly (ethylene glycol)-block-poly(ethylene) amphiphiles. Eur Polym J 72: 270-281.
68. Wang X, Zhang Y, Jiang H, Song Y, Zhou Z, Zhao H (2016) Fabrication and characterization of nano-cellulose aerogels via supercritical CO_2 drying technology. Mater Let 183: 179–182.
69. Zhang H, Bussini D, Hortal M, Elegir G, Mendes J, Jordá Beneyto M (2016) PLA coated paper containing active inorganic nanoparticles: Material characterization and fate of nanoparticles in the paper recycling process. Waste Manage 52: 339–345.

Tables

Table 1. Thickness and basis weight of the films (CNF and CNF/NC) and coated (L2, L3, L4, L5) and uncoated (C60, C80, C120) papers.

Papers/films	Thickness (mm)	Basis weight (g m^{-2})
CNFs	0.015 ± 0.001*	9.6 ± 0.3
CNFs/NC	0.037 ± 0.002	19.4 ± 0.3
L2	0.107 ± 0.002	65.5 ± 0.8
L3	0.126 ± 0.004	85.2 ± 2.7
L4	0.141 ± 0.006	97.2 ± 2.5
L5	0.189 ± 0.006	112.4 ± 8.0
C60 (uncoated)	0.097 ± 0.002	55.2 ± 0.5
C80 (uncoated)	0.124 ± 0.002	73.6 ± 1.0
C120 (uncoated)	0.182 ± 0.002	112.6 ± 1.8

L2: paper coated with CNFs (10 g m^{-2}) L3: paper coated with CNFs (10 g m^{-2}) and CNFs/NC (20 g m^{-2}); L4: paper coated with CNFs (10 g m^{-2}) in both internal and external face and CNFs/NC (30 g m^{-2}) in external face; L5: paper coated with CNFs (10 g m^{-2}) in both internal and external face and CNFs/NC (g m^{-2}) in both internal and external face; C60: 60 g m^{-2}; C80: 80 g m^{-2}; and C120: 120 g m^{-2}; *Standard deviation

Table 2. Basis weight (Bw) and mechanical properties of the different papers (coated: L2, L3, L4, L5; and uncoated: C60, C80, C120).

Papers	Bw (g m^{-2})	TS	TS/Bw	Young's modulus	Young's modulus/Bw	EB	EB/Bw
		(MPa)	(MPa*m^2 g^{-1})	(MPa)	(MPa*m^2 g^{-1})	(mm)	(mm*m^2 g^{-1})
L2	65.5 ± 0.8*	34.5 ± 7.3	0.53 ± 0.11	3,223 ± 150	49.3 ± 2.3	0.04 ± 0.01	0.0006 ± 0.0001
L3	85.2 ± 2.7	39.2 ± 5.5	0.46 ± 0.06	3,436 ± 526	40.3 ± 6.2	0.05 ± 0.01	0.0005 ± 0.0001
L4	97.2 ± 2.5	31.2 ± 2.3	0.32 ± 0.02	2,519 ± 200	22.4 ± 1.8	0.05 ± 0.01	0.0004 ± 0.0001
L5	112.4 ± 8.0	29.6 ± 2.1	0.26 ± 0.02	2,834 ± 359	29.2 ± 3.7	0.06 ± 0.02	0.0006 ± 0.0002
C60 (uncoated)	55.2 ± 0.5	35.2 ± 4.1	0.55 ± 0.07	1,740 ± 108	31.5 ± 2.0	0.10 ± 0.01	0.0017 ± 0.0002
C80 (uncoated)	73.6 ± 1.0	34.7 ± 3.8	0.47 ± 0.05	1,937 ± 192	26.3 ± 2.6	0.10 ± 0.01	0.0017 ± 0.0001
C120 (uncoated)	112.6 ± 1.8	35.6 ± 1.6	0.32 ± 0.01	1,202 ± 329	10.7 ± 2.9	0.20 ± 0.02	0.0014 ± 0.0002

*Standard deviation; Basis weight (Bw); tensile strength (TS); elongation at break (EB); C60: 60 g m^{-2}; C80: 80 g m^{-2}; and C120: 120 g m^{-2};

Table 3. Mechanical properties of the CNF and CNF/NC films.

Film	Tensile strength (MPa)	Elongation at break (mm)	Young's modulus (MPa)
CNFs	24.1 ± 3.3*	0.03 ± 0.02	1,871 ± 14
CNFs/NC	11.9 ± 0.1	0.01 ± 0.00	1,893 ± 238

*Standard deviation

Figures

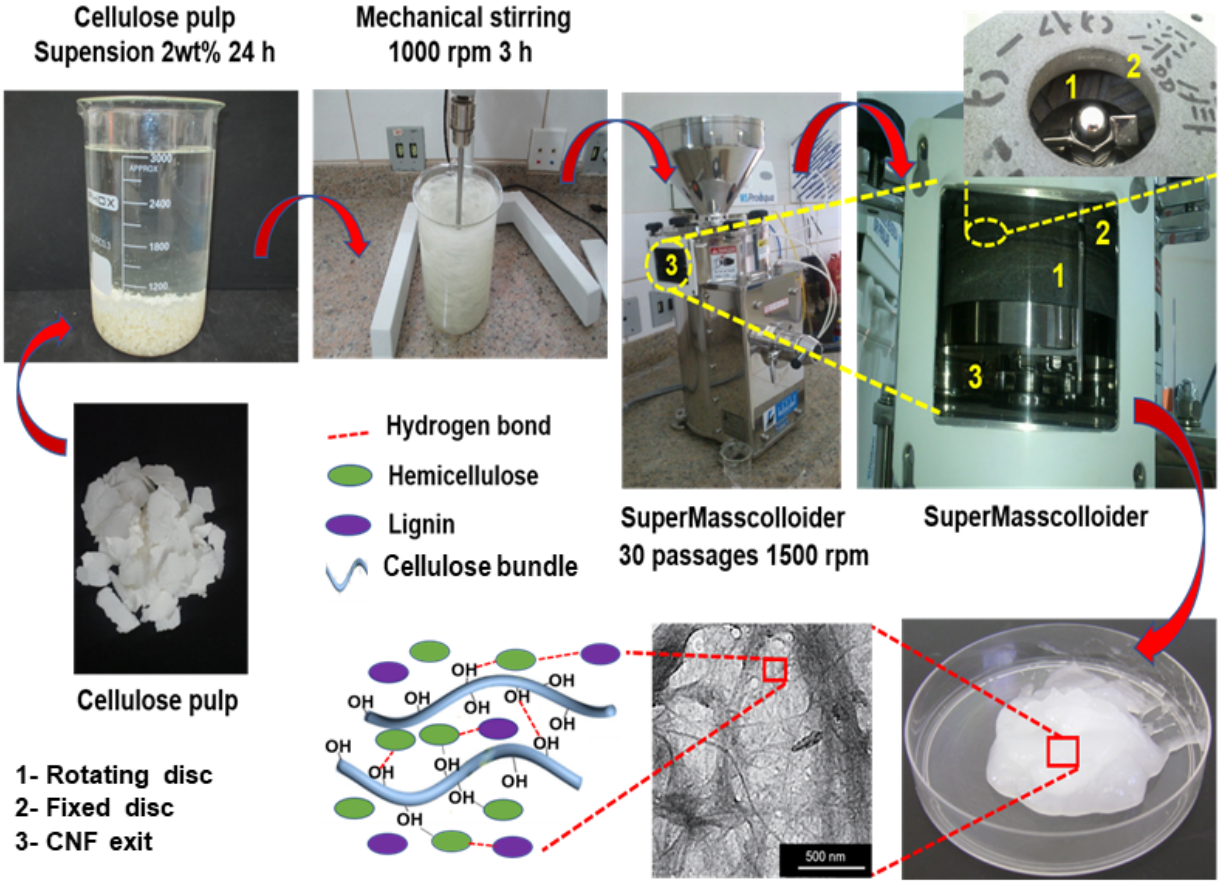

Figure 1

Representative scheme of the production of the CNFs by cellulose fibrillation through the SuperMasscolloider

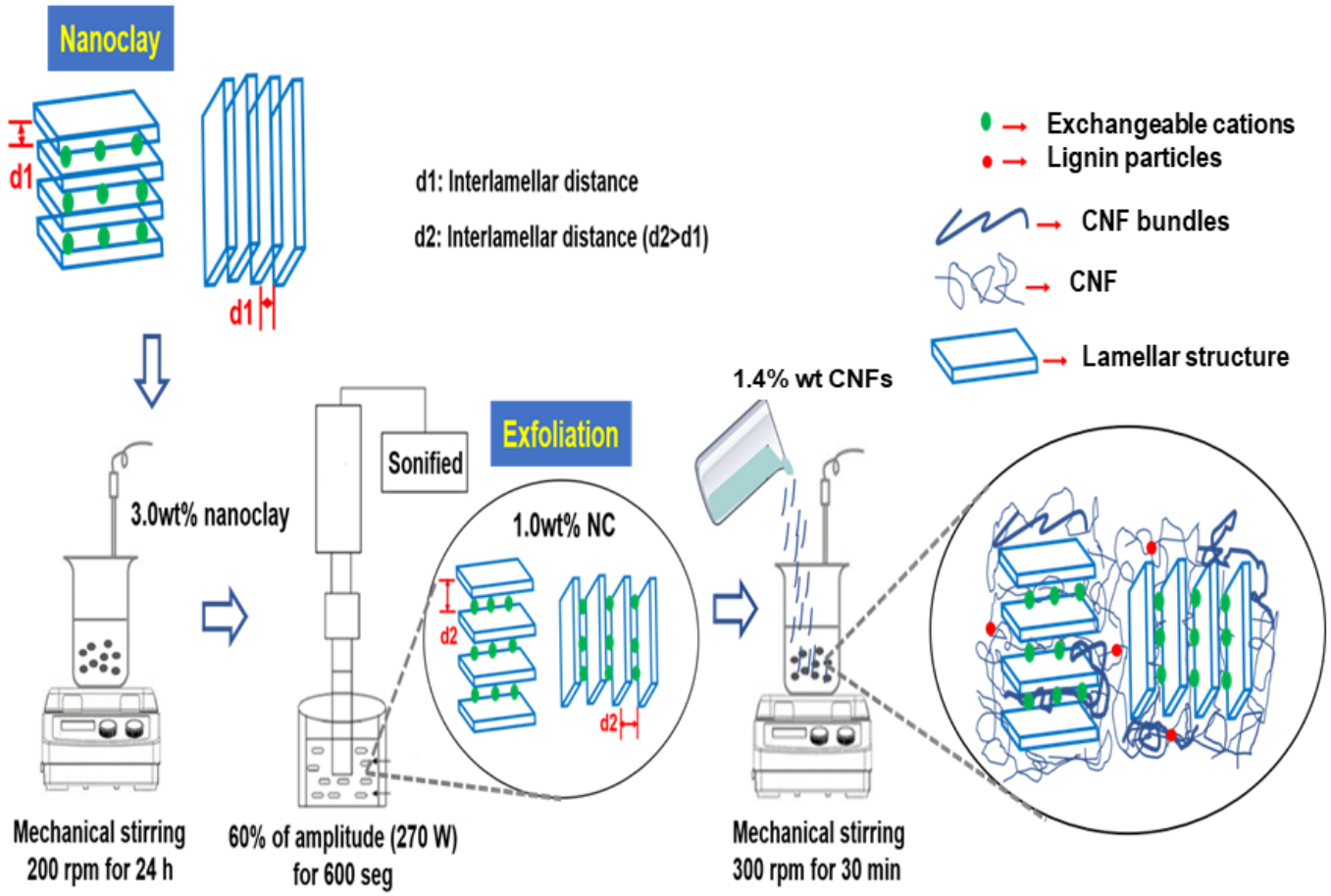

Figure 2

Representative scheme of the exfoliated NC intercalated in the CNF suspension

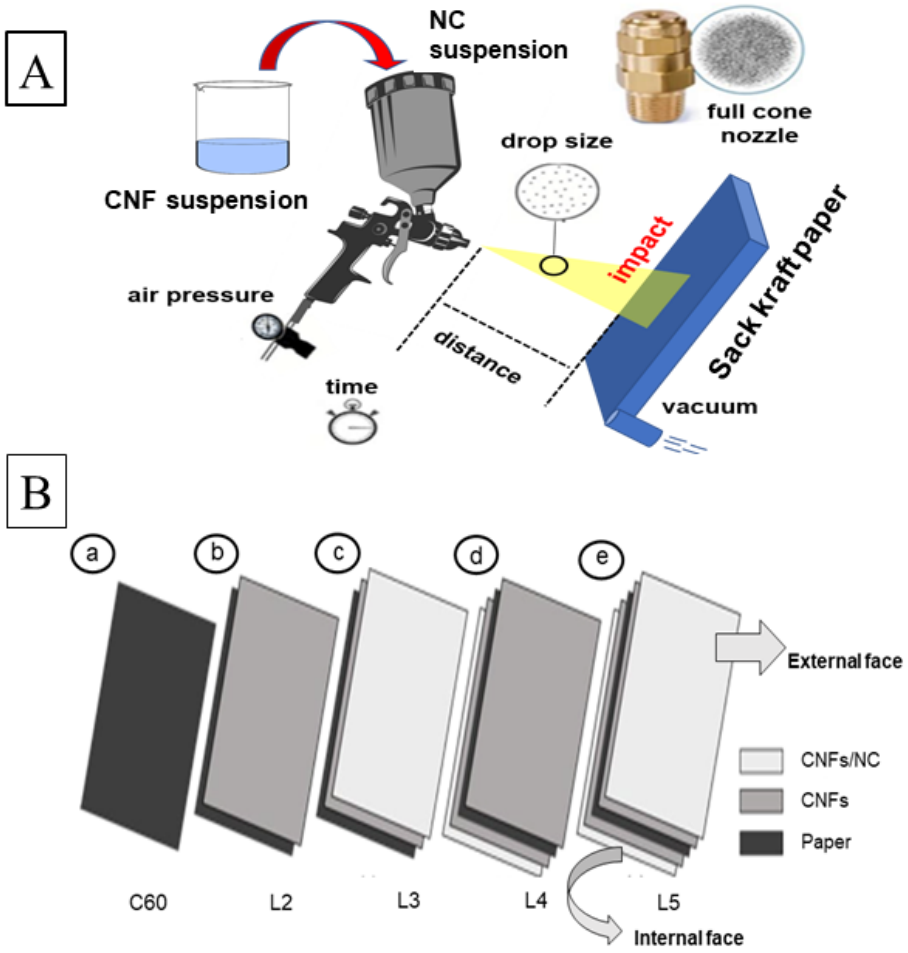

Figure 3

(A) Representative scheme of the spray coating process of the sack kraft paper with CNFs; (B) Representative scheme of uncoated and coated papers: (a) 60 g m-² sack kraft paper (C60); (b) sack kraft paper with CNF layer (10 g m-2) on the external face (L2); (c) sack kraft paper with CNF/NC layer (20 g m-2) applied on the CNF layer (10 g m-2) (L3); (d) sack kraft paper with CNF layer on internal (10 g m-2) and external (10 g m-2), and with one CNF/NC layer (20 g m-2) on the internal surface (L4); and (e) sack kraft paper with internal and external surfaces coated with one layer of CNFs (10 g m-2) applied on both faces (internal and external), and one layer of CNFs/NC (20 g m-2) applied on both faces of the paper (external and internal) on the CNF layers (L5)

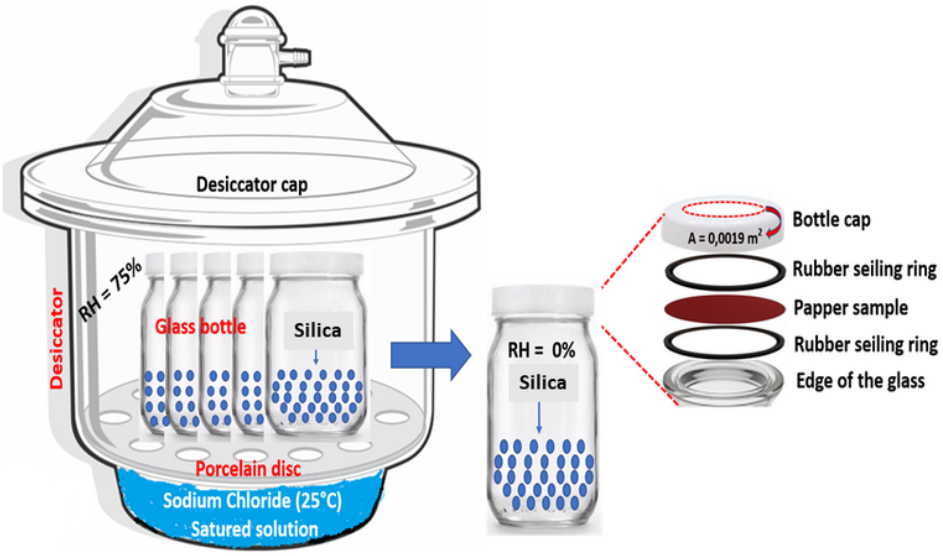

Figure 4

Representative scheme of the apparatus for determination of WVTR

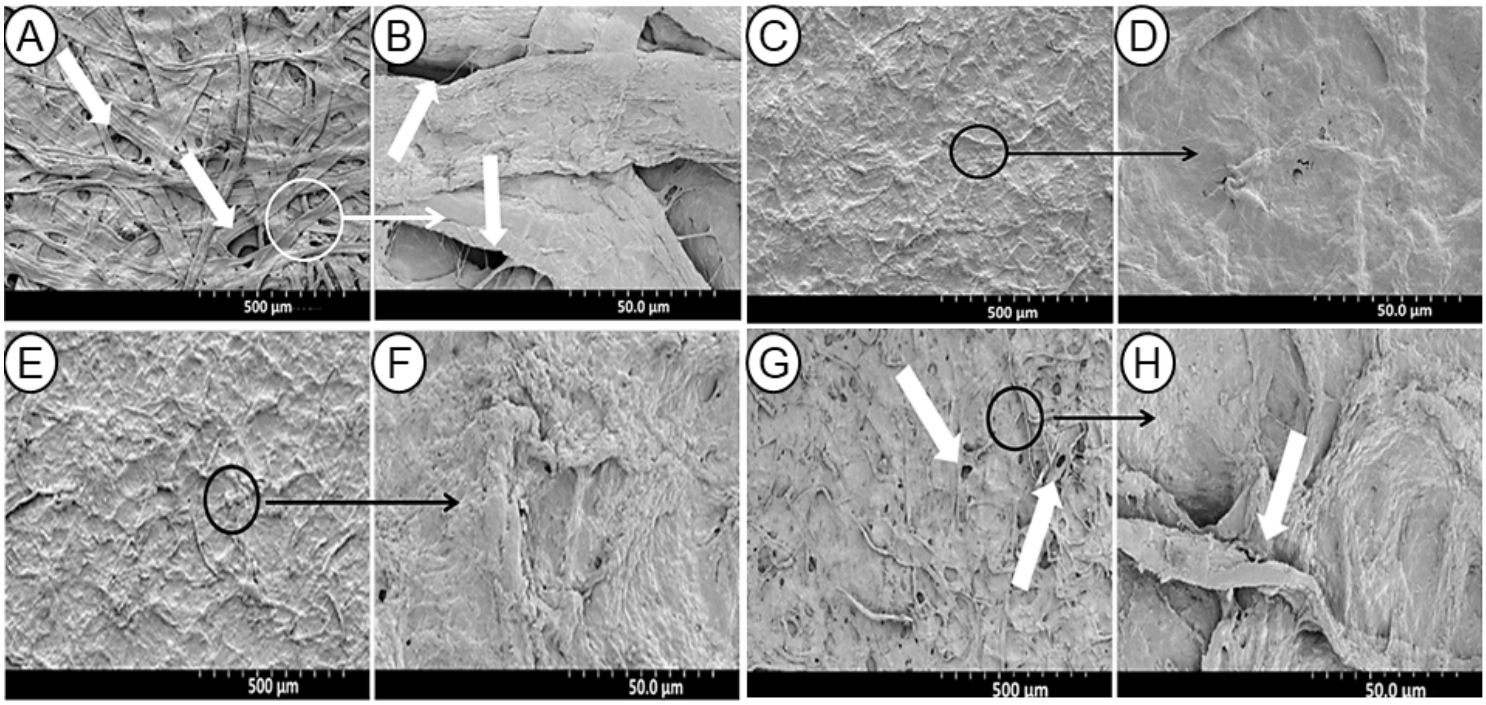

Figure 5

Typical SEM image of the surface of: A and B - uncoated 60 g m-² (C60) sack kraft paper and detail on the paper surface, respectively (white arrows indicate micropores); C and D - coated paper L2 and detail of the coated paper L2 surface, respectively; E and F - coated paper L3 and detail of the coated paper L3 surface, respectively; G and H - coated paper L5 and detail of the most external coated surface (CNFs/NC), respectively: white arrows indicate micropores on the paper surface

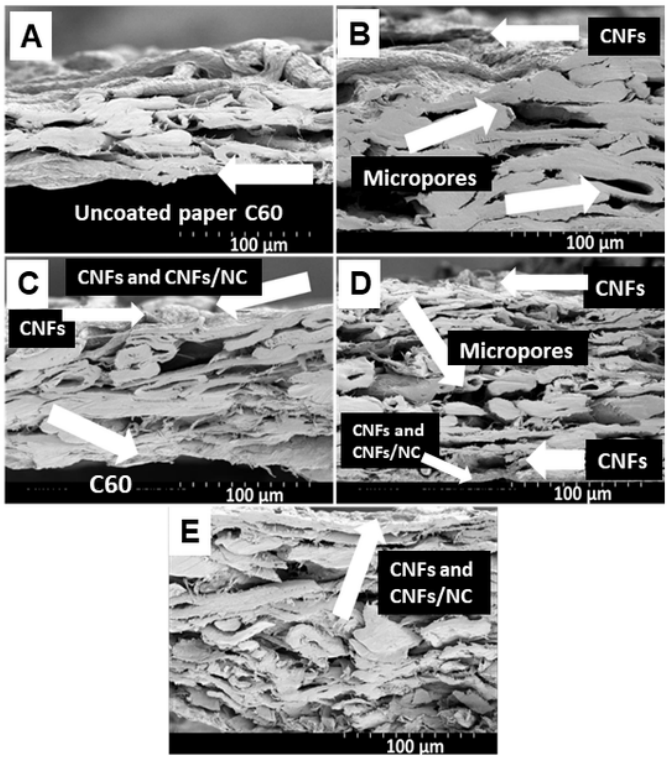

Figure 6

Typical SEM images of the papers cross section: A) uncoated sack kraft paper (C60); B) coated paper L2; C) coated paper L3; D) coated paper L4; E) coated paper L5

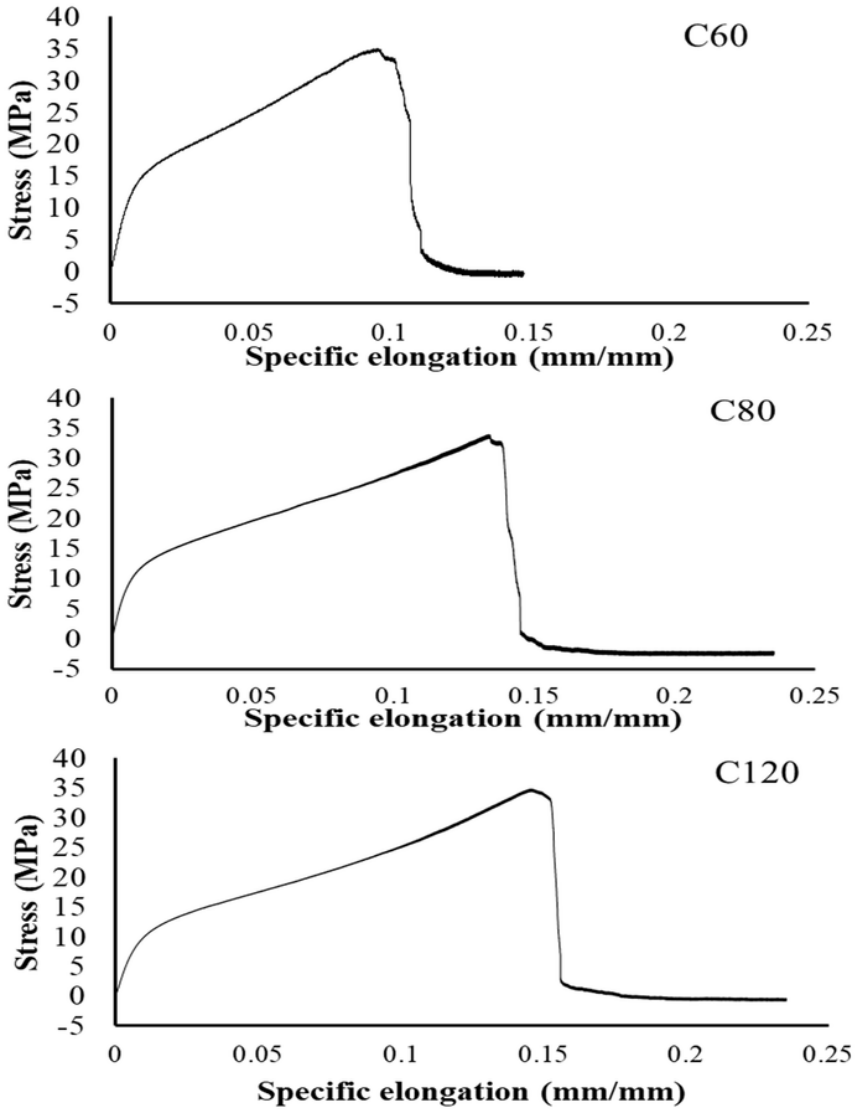

Figure 7

Typical stress x specific elongation curves of uncoated sack kraft papers C60, C80 and C120

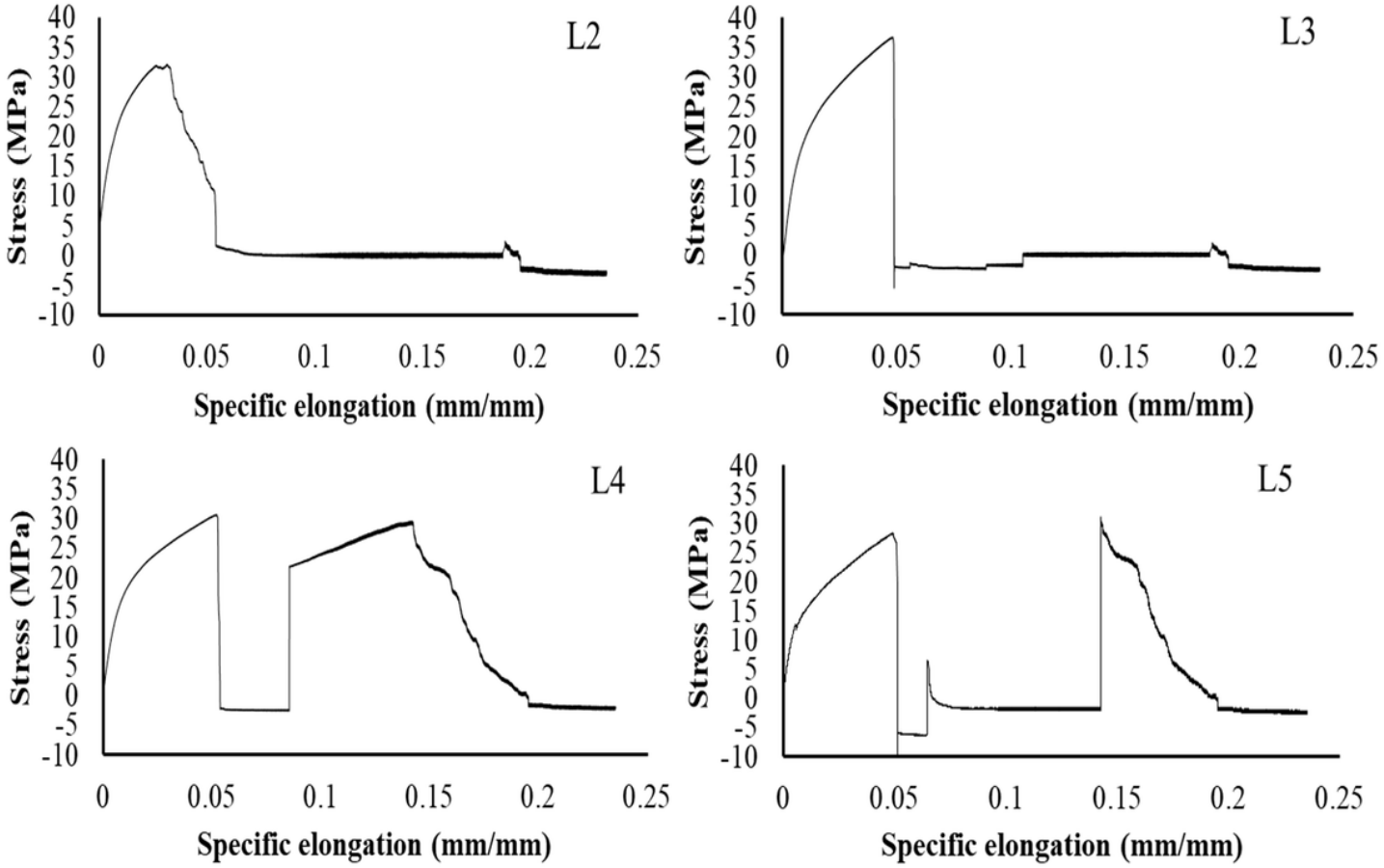

Figure 8

Typical stress x specific elongation curves for the coated papers L2, L3, L4, and L5 papers

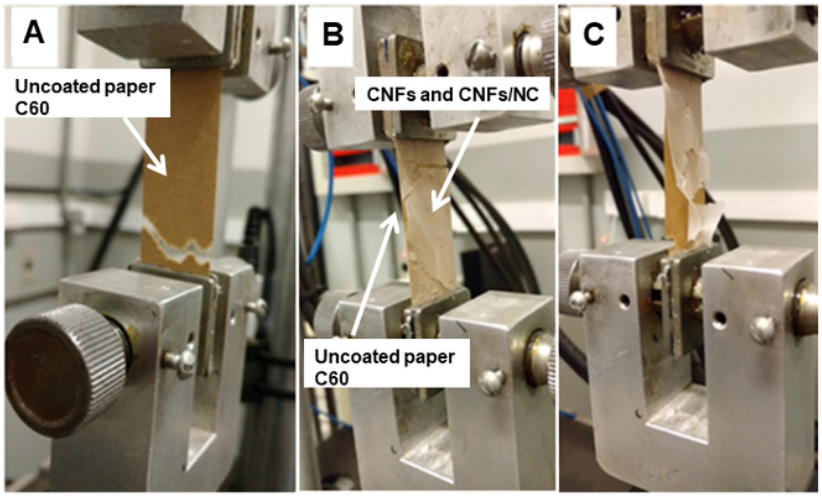

Figure 9

Apparatus for tensile testing showing the rupture of the samples; A) C60 (uncoated paper with 60 g m-2); B) L4 coated paper (the deposited CNF layer ruptured before the paper substrate); and C) L3 coated paper (the deposited CNF layer ruptured before the paper substrate)

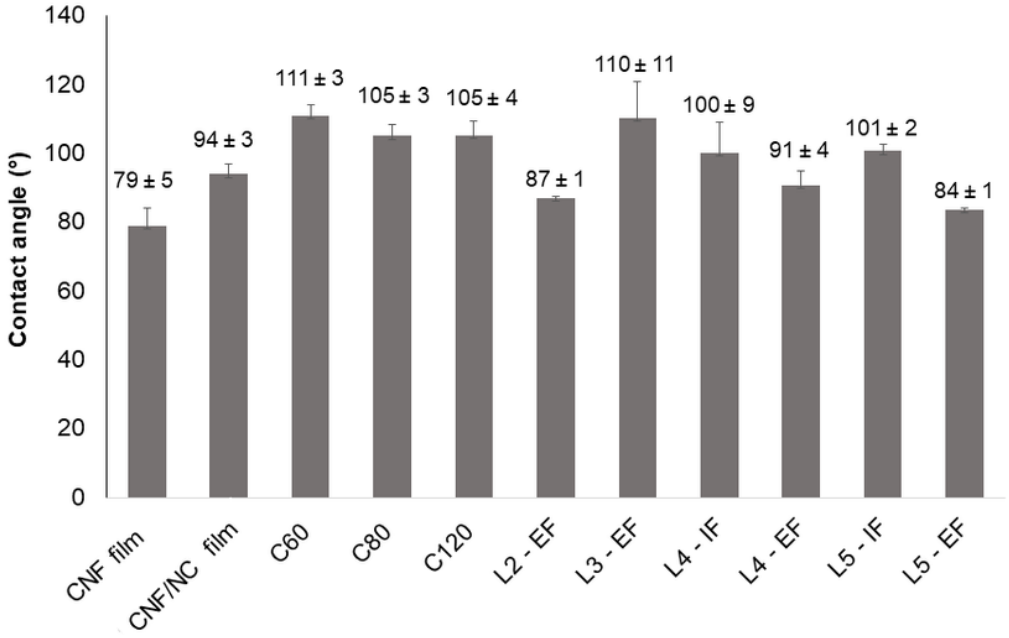

Figure 10

Average and standard deviation values of contact angle for CNF and CNF/NC films, and uncoated (C60, C80 and C120) and coated papers; IF = internal face; EF = external face

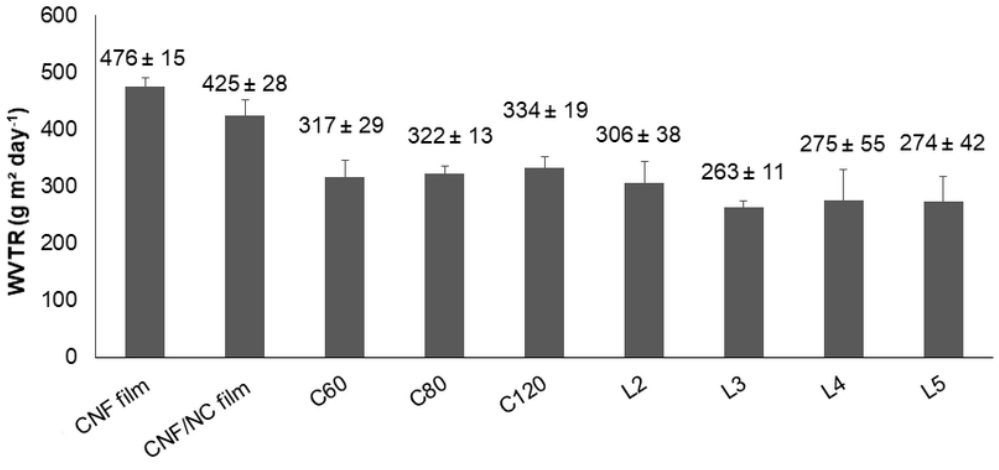

Figure 11

Average values of WVTR for the films and papers produced